Article

Methyl-reducing methanogenesis by a thermophilic culture of Korarchaeia

https://doi.org/10.1038/s41586-024-07829-8

Received: 20 January 2023

Accepted: 15 July 2024

Published online: 24 July 2024

Check for updates

Viola Krukenberg[1,3]✉, Anthony J. Kohtz[1,3], Zackary J. Jay[1] & Roland Hatzenpichler[1,2]✉

Methanogenesis mediated by archaea is the main source of methane, a strong greenhouse gas, and thus is critical for understanding Earth's climate dynamics. Recently, genes encoding diverse methanogenesis pathways have been discovered in metagenome-assembled genomes affiliated with several archaeal phyla[1–7]. However, all experimental studies on methanogens are at present restricted to cultured representatives of the Euryarchaeota. Here we show methanogenic growth by a member of the lineage Korarchaeia within the phylum Thermoproteota (TACK superphylum)[5–7]. Following enrichment cultivation of '*Candidatus* Methanodesulfokora washburnenis' strain LCB3, we used measurements of metabolic activity and isotope tracer conversion to demonstrate methanol reduction to methane using hydrogen as an electron donor. Analysis of the archaeon's circular genome and transcriptome revealed unique modifications in the energy conservation pathways linked to methanogenesis, including enzyme complexes involved in hydrogen and sulfur metabolism. The cultivation and characterization of this new group of archaea is critical for a deeper evaluation of the diversity, physiology and biochemistry of methanogens.

Methane is a potent greenhouse gas, and its atmospheric levels contribute to the regulation of Earth's climate. Most methane (roughly 58–64%) is generated in anoxic environments by methanogenic archaea[8,9] in a strictly anaerobic process called methanogenesis[10]. These microorganisms play a critical role in the global carbon cycle by catalysing the final step in organic matter degradation and are of high interest for biotechnological applications including the production of methane as an energy source[11]. Methanogens use compounds such as CO_2–H_2, acetate or methanol, and the enzymatic pathways leading to methane formation differ depending on the substrate[10,12]. However, all methanogens use the methyl-coenzyme M reductase (MCR) complex for the final conversion of methyl-coenzyme M and coenzyme B into methane and the CoM-S-S-CoB heterodisulfide[13]. This key enzyme also catalyses the reversible reaction in the anaerobic oxidation of methane and other alkanes in alkanotrophic archaea[13,14]. The isolation of methanogens into axenic cultures has been fundamental to decades of research on their physiology and biochemistry[15]. So far, methanogenesis has exclusively been studied in lineages of the Euryarchaeota, and no methanogen from outside this superphylum has ever been cultured for experimental investigation. Only recently have environmental metagenomic studies identified genes of the methanogenesis pathway, including those in the MCR complex, to be encoded by archaea across several new lineages[1–7]. These newly proposed groups of methanogenic archaea could have important but so far unrecognized environmental effects or hold undiscovered biotechnological potential.

'*Ca*. Methanodesulfokora washburnensis', formerly '*Ca*. Methanodesulfokores washburnensis'[7,16], was first identified as a potential methanogen by metagenome-assembled genomes (MAGs) obtained from Washburn Hot Springs (WHS) in Yellowstone National Park (YNP) (Wyoming, USA)[5–7]. Metabolic reconstruction predicted methyl-reducing hydrogen-dependent methanogenesis among other possible respiratory pathways, including anaerobic oxidation of methane and sulfite reduction[5–7]. Its unique metabolic potential at the intersection of carbon and sulfur cycling[5–7], together with its deeply branching phylogenetic position within the phylum Thermoproteota (formerly the TACK superphylum), make this archaeon a prime candidate for culture-dependent research into the physiology, biochemistry and metabolic versatility of methanogens.

Here, we combined selective cultivation with fluorescence microscopy, growth experiments, and metagenome and metatranscriptome sequencing to demonstrate methyl-reducing methanogenesis by a thermophilic culture of this korarchaeon.

Methanogenic enrichments

So far, '*Ca*. Methanodesulfokora'-related 16S ribosomal RNA (rRNA) genes have been detected almost exclusively in terrestrial geothermal systems, including in hot spring metagenomes from YNP ($n = 7$), New Zealand ($n = 1$) and Kamchatka ($n = 1$) (Supplementary Tables 1 and 2). Consistently, '*Ca*. Methanodesulfokora' *mcrA* gene sequences have been detected only in metagenome assemblies from geothermal environments in YNP[5,7,17,18] (Supplementary Table 3). We selected WHS and two hot springs in the Lower Culex Basin (LCB003 and LCB058) of YNP as source materials for cultivation. These hot springs ranged in

[1]Department of Chemistry and Biochemistry, Center for Biofilm Engineering, and Thermal Biology Institute, Montana State University, Bozeman, MT, USA. [2]Department of Microbiology and Cell Biology, Montana State University, Bozeman, MT, USA. [3]These authors contributed equally: Viola Krukenberg, Anthony J. Kohtz. ✉e-mail: viola.krukenberg@montana.edu; roland.hatzenpichler@montana.edu

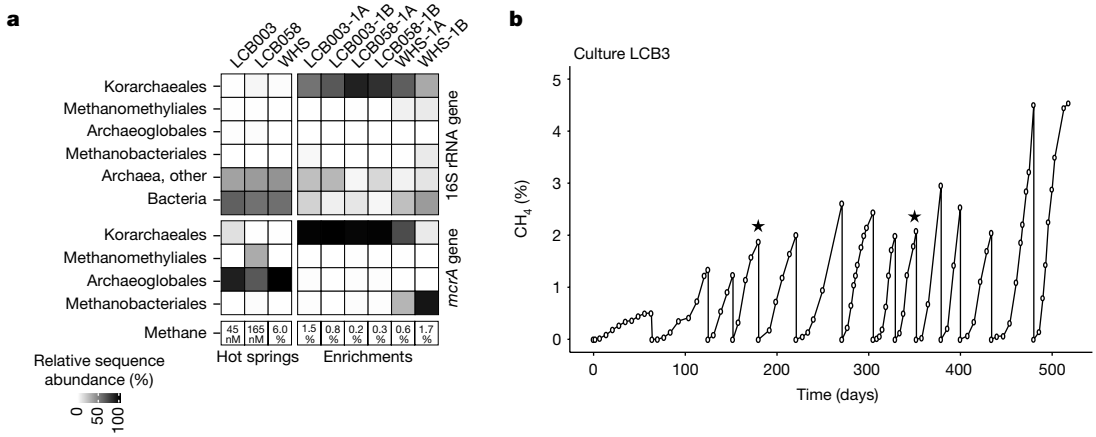

Fig. 1 | Methane-producing enrichment cultures from hot spring sediments. a, Relative abundance of Korarchaeales in hot spring sediments and in enrichments after 64–67 days of incubation as inferred by amplicon sequencing of *mcrA* and 16S rRNA genes. Enrichments were established from hot springs in the LCB (LCB003, LCB058) and WHS thermal areas. Enrichments were supplied with methanol and hydrogen in the absence (1A) or presence (1B) of antibiotics. Shading is proportional to relative sequence abundance (%). Lineages containing MCR-encoding archaea are depicted on order level, relative abundances more than 1% are shown. Methane values for hot springs LCB003 and LCB058 (ref. 17) refer to dissolved methane; methane value for WHS[7] and methane values for enrichments refer to the precentage of methane measured in the headspace. **b**, Headspace methane development of culture LCB3 initiated with sediment material from hot spring LCB003 (days 0–64) and maintained in anoxic media (days 65–518) amended with methanol plus hydrogen and antibiotics. See Supplementary Table 5 for details. Stars indicate time points at which metagenome sequencing was performed.

temperature (64–77 °C) and pH (6.1–6.5) and varied in the relative abundance of Korarchaeales-related 16S rRNA gene amplicons (0.4–3.6%; Fig. 1a, Extended Data Fig. 1 and Supplementary Table 4). From each hot spring, anoxic incubations of sediment slurries were conducted at in situ temperature (WHS, 64 °C; LCB003, 77 °C; LCB058, 70 °C) and supplied with methanol and hydrogen in the presence or absence of antibiotics (Supplementary Table 5). Within 64 to 67 days of incubation we detected a strong increase in the relative abundance of both 16S rRNA and *mcrA* gene amplicons identified as '*Ca*. M. washburnensis' (Supplementary Tables 4 and 5). '*Ca*. M. washburnensis' dominated the microbial community of all incubations, constituting up to 86% relative abundance while other MCR-encoding archaea affiliated with Methanomethyliales, Archaeoglobales and Methanobacteriales were also detected (more than 1% relative abundance). All incubations showed methane production (Fig. 1a and Supplementary Table 5), with incubation LCB003-1B containing near-exclusively *mcrA* gene amplicons related to '*Ca*. M. washburnensis' (Korarchaeales, more than 99.9% relative abundance). The highest methane levels were observed in incubations WHS-1B and LCB003-1A, in which, on the basis of 16S rRNA gene amplicon sequencing, both '*Ca*. M. washburnensis' and a *Methanothermobacter* sp. were detected. *Methanothermobacter* spp. are thermophilic, obligate CO_2-reducing hydrogenotrophic methanogens that previously had been isolated from geothermal environments of YNP[19,20].

As inoculum for continued cultivation of '*Ca*. M. washburnensis', we selected a replicate of the methanogenic enrichment LCB003-1B (Supplementary Tables 4 and 5). The microbial community of this enrichment lacked previously cultured Euryarchaeotal methanogens (less than 0.1% relative abundance of 16S rRNA gene amplicons) and was dominated by '*Ca*. M. washburnensis' (66.6 and 99.9% relative abundance of 16S rRNA and *mcrA* gene amplicons, respectively).

Cultivation and genome recovery

For selective cultivation, we designed a medium according to the growth requirements for hydrogen-dependent methyl-reducing methanogenesis predicted from metabolic reconstructions of '*Ca*. M. washburnensis' MAGs[5–7]. Methanol (10 mM) and hydrogen (50%) were supplied as methanogenic substrates, antibiotics were amended to reduce bacterial growth and incubation was conducted at in situ temperature of 77 °C. Activity was monitored by measuring methane concentrations in the headspace and cultures were transferred at late exponential phase of methane production. Continuous transfers of the active methanogenic culture into fresh media resulted in a sediment-free culture, designated culture LCB3. During 13 continuous cultivation cycles (that is, transfers; more than 500 days total) the final methane concentration and methane production rate increased steadily from a maximum of 2 to 5% headspace gas, equivalent to about 2 mM of methane, and from roughly 63 to 38 days, respectively (Fig. 1b). The growth temperature of culture LCB3 is well above that of other cultured methanol-using methanogens[21,22] and near the boiling point of methanol (84 °C at 200 kPa), which probably reduced the amount of methanol effectively available in the liquid medium.

Metagenome long-read sequencing (PacBio) performed on culture LCB3 (day 352, Fig. 1b) resulted in the recovery of a complete, closed chromosome that was highly related to previously obtained '*Ca*. M. washburnensis' MAGs (NM4, LMO9 and MDKW; Supplementary Table 6)[5–7] on the basis of average nucleotide and amino acid identities (97–98%; Extended Data Fig. 2a), phylogenomic reconstruction (Fig. 2a, Extended Data Fig. 3a and Supplementary Table 7) and 16S rRNA gene identity and phylogeny (99%; Extended Data Fig. 3b). We thus designate the archaeon enriched here as '*Ca*. M. washburnensis' strain LCB3. The genome of strain LCB3 is similar in size and number of coding sequences to the MAG of '*Ca*. M. washburnensis' NM4 and the genome of '*Ca*. Korarchaeum cryptofilum' OPF8, but notably smaller than the MAGs of both '*Ca*. M. washburnensis' MDKW and LMO9 (Supplementary Table 6). MAGs NM4, MDKW and LMO9 were independently recovered from the same metagenome dataset of WHS but processed by different bioinformatic methods[5–7]. The variation in MAGs from WHS together with the genome size of strain LCB3, suggests that the '*Ca*. M. washburnensis' population in WHS could consist of several strains. We estimate the abundance of strain LCB3 in its native hot spring environments of WHS, LCB003, and LCB058 between 0.1 and 2.9% on the basis of mapping of metagenomic short reads to its genome. Metagenome short-read sequencing (Illumina) performed on culture LCB3 at two time points (days 180 and 352, Fig. 1b) showed an enrichment of 62–82% of '*Ca*. M. washburnensis' (Fig. 2b and Extended Data Fig. 2b). Other community members in culture LCB3 included *Archaeoglobaceae*, *Thermofilum*, *Fervidicoccaceae*, *Ignisphaera* and *Desulfurococcaceae* (Fig. 2b and Extended Data Fig. 3b), for which

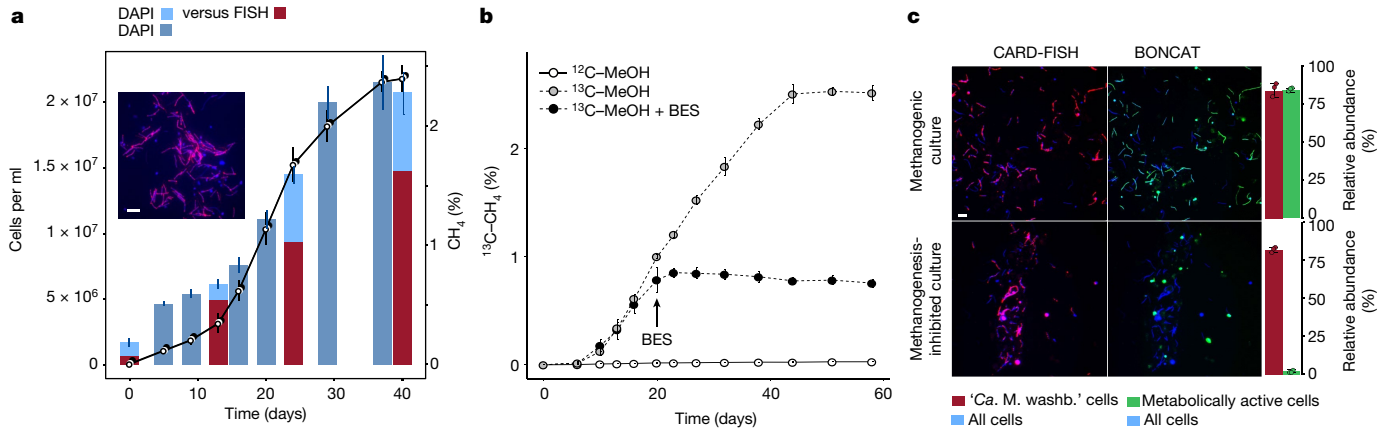

Fig. 2 | Growth and translational activity of culture LCB3. a, Development of methane concentration and cell number. Relative abundance of '*Ca*. M. washburnensis' cells was determined at four time points (day 0, 12, 24, 40) on the basis of the fraction of '*Ca*. M. washburnensis'-specific FISH counts (red) versus total counts of DAPI-stained cells (blue). Data are presented as mean ± s.d. ($n = 4$ biological replicates). Representative micrograph from $n = 4$ biological replicate cultures. **b**, Production of ^{13}C-methane in cultures amended with ^{12}C-methanol (open symbols, solid line) or ^{13}C-methanol (grey symbols, dashed line). No ^{13}C enrichment of methane was detected in cultures amended with ^{12}C-methanol. BES addition to active cultures resulted in the inhibition of methanogenesis (black circles, dashed line). Data are presented as mean values ± standard deviation ($n = 3$ biological replicates). **c**, Anabolic activity of cells in culture LCB3 visualized through BONCAT (green), combined with CARD-FISH (red) to identify '*Ca*. M. washburnensis' cells. '*Ca*. M. washburnensis' cells were translationally active in a methane-producing culture but not in a culture in which methanogenesis was inhibited with BES. In methanogenic cultures BONCAT-labelled cells (green bar) and CARD-FISH-labelled cells (red bar) each accounted for 84% of all DAPI-stained cells. In methanogenesis-inhibited cultures BONCAT-labelled cells accounted for 2% whereas CARD-FISH-labelled cells accounted for 82%. This suggests that anabolic activity of '*Ca*. M. washburnensis' cells ceased when methanogenesis was inhibited. Representative micrographs from $n = 3$ biological replicate cultures. Scale bars, 5 µm.

circular genomes were also recovered (Supplementary Table 8). Consistently, application of a general archaeal catalysed reporter deposition fluorescence in situ hybridization (CARD-FISH) probe revealed filamentous and coccus-shaped cells, whereas no cells were identified with general bacterial probes (Fig. 2b, Extended Data Fig. 4 and Supplementary Table 9).

The only *mcr* genes (*mcrABG*) identified in the metagenomes from culture LCB3 at both time points belong to the genome of strain LCB3. Phylogenetic analysis of the McrA revealed that it is highly related to previously recovered McrA from Korarchaeia MAGs and an McrA from a sediment metagenome of hot spring LCB003 (Fig. 2c), which had served as source material for culture LCB3. This is strong evidence that strain LCB3 is the only methanogen in the culture.

Metabolic activity on methanol and H_2

FISH on culture LCB3 using a probe specific for the 16S rRNA of '*Ca*. M. washburnensis' revealed abundant filamentous cells (Fig. 3a, Extended Data Fig. 4 and Supplementary Table 9), similar in morphology to the previously described non-methanogenic '*Ca*. K. cryptofilum' OPF8 (ref. 23). Filaments varied in lengths between roughly 3 to more than 20 µm, and filaments were observed both individually and in cell aggregates. We tracked the growth of strain LCB3 by CARD-FISH. This showed that its relative cell abundance increased with methane production from roughly 30% during lag phase to 70% during log phase (Fig. 3a). On the basis of cell counts, the total cell density of culture LCB3 reached 2×10^7 cells per ml with an estimated doubling time of 6 days. By growing culture LCB3 in the presence of ^{13}C-methanol and measuring the transfer of isotopic label to ^{13}C-methane, we confirmed that methanol was converted to methane (Fig. 3b and Extended Data Fig. 5a). Methane production ceased on addition of bromoethanesulfonate (BES), an inhibitor of the MCR complex. Methane production and growth of strain LCB3 were not sustained without amendment of methanol. Mono-, di- and trimethylamine as well as higher chain alcohols (ethanol and isopropanol) did not support methanogenic growth of strain LCB3 (Extended Data Fig. 5c).

To demonstrate that translational activity is coupled to methanogenesis in strain LCB3, we evaluated its metabolic activity under methanogenic and methanogenesis-inhibited conditions using a combination of bioorthogonal non-canonical amino acid tagging (BONCAT) and FISH. For this, two replicate culture sets were grown to exponential phase, at which point one set was inhibited with BES before both sets were spiked with the amino acid analogue L-homopropargylglycine (HPG) to trace translationally active cells (Extended Data Fig. 5b). We visualized cells of '*Ca*. M. washburnensis' by means of CARD-FISH and identified anabolically active cells through click chemistry mediated dye-staining. On the basis of cell counts, '*Ca*. M. washburnensis' accounted for roughly 80% of the cells in both culture sets, whereas BONCAT-labelling revealed anabolic activity of '*Ca*. M. washburnensis' cells under only methanogenic conditions (Fig. 3c). This indicated that translational activity is dependent on the activity of the MCR complex. Thus, we present experimental evidence that a representative of the Korarchaeia grows by methanogenesis.

Gene expression during methanogenesis

To reveal the mechanisms involved in methyl-reducing methanogenesis in strain LCB3 we analysed its genome and studied its gene expression during growth with methanol and hydrogen (Fig. 4, Extended Data Fig. 6 and Supplementary Tables 10 and 11). Notably, metatranscriptome sequencing conducted on culture LCB3 showed that 98% of the reads mapped to the genome of strain LCB3. Strain LCB3 highly expressed the Mcr complex (*mcrABGCD*) and the methanol:coenzyme M methyltransferase system (*mtaABC*) that are both required for the conversion of methanol to methane and a heterodisulfide (CoM-S-S-CoB)[10,12]. However, the genome did not encode the methyltetrahydromethanopterin:coenzyme M methyltransferase (Mtr) complex and the methyl-branch of the Wood–Ljungdahl pathway (Fig. 4a and Supplementary Table 10). This supports the idea that methanogenesis in strain LCB3 is based on methyl-reduction rather than methyl-disproportionation into methane and carbon dioxide. Consequently, strain LCB3 relies on the oxidation of an electron donor, such as hydrogen, for the reduction of

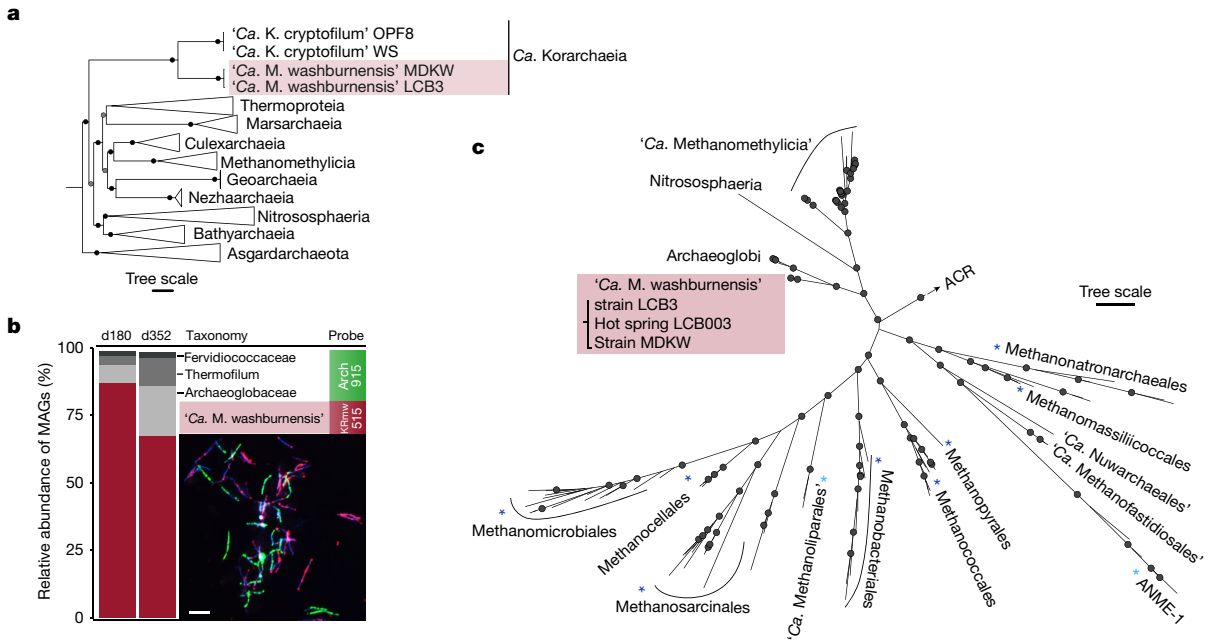

Fig. 3 | Phylogenetic affiliation of '*Ca*. M. washburnensis' strain LCB3. **a**, Phylogenetic reconstruction based on 33 single-copy marker genes showing affiliation of strain LCB3 with representative Korarchaeia genomes and MAGs. **b**, Composition of culture LCB3 based on relative abundance of recovered genomes (relative abundance more than 1%, $n = 1$ metagenome), and visualization of korarchaeal (red) and other archaeal cells (green) by CARD-FISH. Representative micrograph from $n = 3$ independent samples from culture LCB3. Note that because of two central mismatches between the 16S rRNA of '*Ca*. M. washburnensis' and the archaea-specific probe (Arch915), no dual labelling of '*Ca*. M. washburnensis' was observed. **c**, Phylogenetic tree of McrA showing the close affiliation of McrA from '*Ca*. M. washburnensis' strain LCB3 with McrA from strain MDKW and McrA from the metagenome of hot spring LCB003. Asterisks indicate lineages with availability of methanogenic or methanotrophic isolates (dark blue) or enrichment cultures (light blue), which all belong to the superphylum Euryarchaeota. Circles represent bootstrap support values more than 95. ACR, alkyl-coenzyme M reductase. Scale bar, 5 µm (**b**); tree scales, 0.2 (**a**), 0.1 (**c**).

CoM-S-S-CoB, as previously discussed for related MAGs[5–7]. All previous metabolic inferences suggested an energy conservation mechanism by means of a soluble electron-bifurcating hydrogenase–heterodisulfide reductase complex (Mvh–Hdr) coupled to a Fpo-like–HdrD complex[5–7]. Whereas strain LCB3 expressed the Fpo-like complex (Fig. 4, Extended Data Fig. 7b and Supplementary Table 11) and HdrD subunits, no genes encoding an Mvh–Hdr complex were identified, which suggests an alternative route for linking hydrogen oxidation and CoM-S-S-CoB reduction. Metabolic reconstruction supported by transcriptional activity suggest that in strain LCB3 hydrogen is oxidized by a membrane-bound [NiFe]-hydrogenase of group 1g (ref. 24), and electrons are transferred through a membrane-bound electron carrier to an integral membrane b-type cytochrome containing heterodisulfide reductase complex (HdrDE) that catalyses the cytoplasmic reduction of CoM-S-S-CoB (Fig. 4b, Extended Data Figs. 7a and 8 and Supplementary Table 11). Different from previously characterized group 1 [NiFe]-hydrogenases of the 1k or 1j type (Vht or Vho, respectively) in methanogens, the group 1g [NiFe]-hydrogenase complex encoded in the LCB3 genome does not contain a cytochrome b subunit (Extended Data Fig. 7a). Instead, it includes two proteins with similarity to NrfC and NrfD families (Extended Data Fig. 8a), which could substitute for the function of cytochrome b in reducing a membrane-bound electron carrier[25]. Group 1g [NiFe]-hydrogenases have not been previously linked to methanogenesis and may present a unique Korarchaeia-specific differentiation in the enzymatic machinery of methanogens. Energy conservation during hydrogen-dependent methyl-reducing methanogenesis could thus rely on a simple respiratory chain of membrane-bound group 1g [NiFe]-hydrogenase and b-type cytochrome (HdrE), in which both enzyme complexes would contribute to establishing an ion gradient used for the synthesis of ATP through a V-type ATP synthase (Fig. 4). Strain LCB3 also expressed a long-chain geranylfarnesyl diphosphate synthase related to sequences from *Methanosarcina*, *Archaeoglobus* and Methylarchaeles (Extended Data Fig. 9 and Supplementary Table 11), suggesting strain LCB3 may synthesize methanophenazine[26]. Furthermore, variable expression levels of enzymes putatively involved in menaquinone biosynthesis (Supplementary Table 11) indicate a potential to produce diverse membrane-bound electron carriers. Notably, c-type cytochromes were not encoded in the LCB3 genome.

Along with the pathway for hydrogen-dependent methanol-reducing methanogenesis, the transcriptional profile of strain LCB3 revealed several other enzymes possibly linked to methanogenesis. In addition to the methanol:coenzyme M methyltransferase system (*mtaABC*) for methanol reduction, homologues of a trimethylamine methyltransferase, MttB, and an associated corrinoid protein, MttC, were highly expressed. Proteins in the MttB family have been shown to catalyse the demethylation of a variety of substrates[27–29]. Low sequence similarity to characterized MttBC homologues along with the absence of growth on trimethylamine, suggests that this represents a new, yet uncharacterized methyltransferase system. Strain LCB3 also expressed a new group 4 [NiFe]-hydrogenase, termed here Ehi. This complex could catalyse the reversible oxidation of hydrogen at the expenditure of an ion gradient to produce reduced ferredoxin[30] for CoM-S-S-CoB reduction, akin to the functional role of Ech or Ehb-type hydrogenases in Euryarchaeotal methanogens[15]. Similar to Fpo, Ehi may form a complex with HdrD, allowing for coupling the direct oxidation of hydrogen to the reduction of CoM-S-S-CoB and ion translocation. Furthermore, a membrane-bound group 4b [NiFe]-hydrogenase–carbon monoxide dehydrogenase complex provides the potential to couple the oxidation of carbon monoxide to the internal production of hydrogen and ion translocation[31,32]. However, three subunits of the hydrogenase module (including the catalytic subunit) showed low expression relative to the subunits of the carbon monoxide dehydrogenase and ion transporter modules, suggesting these genes may be differentially regulated, as has been shown in *Thermococcus*[32,33] (Fig. 4b). Similar to

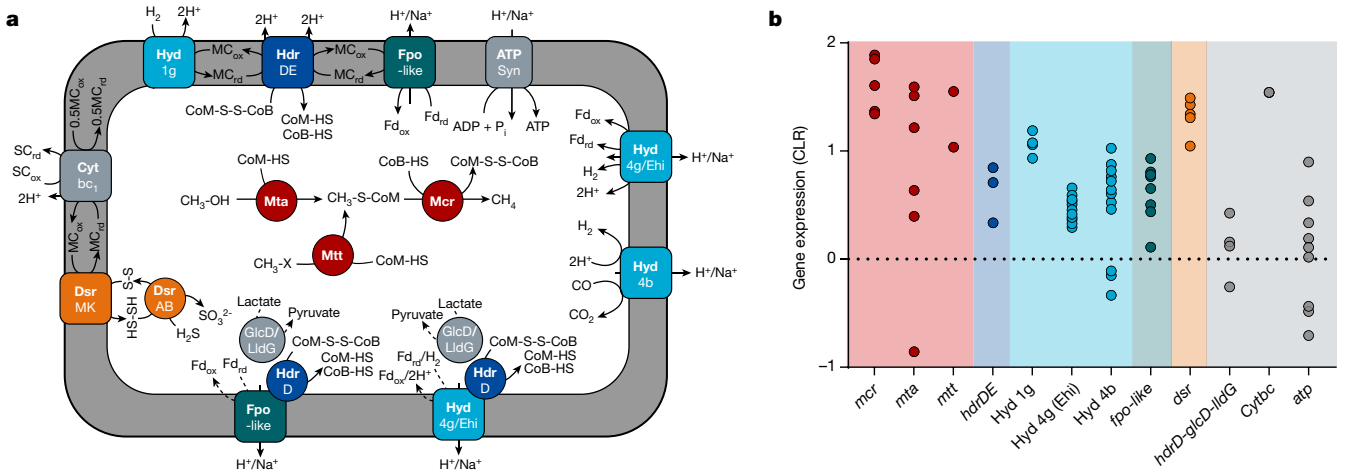

Fig. 4 | Metabolic reconstruction and gene expression of '*Ca*. M. washburnensis' strain LCB3. a, Methanogenesis pathway and possible alternative energy-conserving processes with linkage to methanogenesis. Dashed lines represent alternative reactions, colour-coding differentiates proteins from protein complexes. **b**, Gene expression presented as centre log ratio (CLR) during methanogenic growth on methanol and hydrogen ($n = 1$ experiment). Dotted line represents the geometric mean expression of all genes. Each dot represents the expression of a subunit in a multi-subunit enzyme complex. See Supplementary Tables 10 and 11 for details on gene annotation and gene expression. ATP Syn, ATP synthase; Dsr, dissimilatory sulfite reductase; Fd, ferredoxin; Fpo, F_{420}:methanophenazine oxidoreductase; Glc, lactate dehydrogenase; Hdr, heterodisulfide reductase; Hyd, [NiFe]-hydrogenase; Mcr, MCR; Mta, methanol:coenzyme M methyltransferase; MC, membrane-bound electron carrier; SC, soluble electron carrier; ox, oxidized form; rd, reduced form.

other MCR-encoding archaea within the Thermoproteota, strain LCB3 encoded genes with homology to lactate dehydrogenases, GlcD and LldG that were each colocated with an HdrD and showed low to moderate expression levels. When supplemented with lactate, methane production of culture LCB3 improved, even without added hydrogen (Extended Data Fig. 5c). This could indicate that lactate oxidation by GlcD may contribute electrons to HdrD for the reduction of CoM-S-S-CoB[2,3] coupled to the translocation of ions at either a Fpo-like or Ehi complex, a mechanism previously suggested but not described in any cultured methanogens[2,3]. However, methane production also occurred when culture LCB3 was supplemented only with methanol, with lower yields than with methanol plus hydrogen (Extended Data Fig. 5c). Therefore, we cannot exclude that trace hydrogen was produced by strain LCB3 or co-enriched archaea, or that hydrogen played an intermediate role in lactate metabolism. Notably, a cluster of genes encoding cytoplasmic and membrane-bound components of the (dissimilatory) sulfite reductase system (DsrABCMK) and a cytochrome bc1-like complex was highly expressed. The growth medium of strain LCB3 was supplemented with reduced sulfur species and the dissimilatory sulfite reductase system may function in reverse to couple sulfide oxidation with CoM-S-S-CoB reduction and energy conservation as previously speculated for '*Ca*. M. washburnensis' MKDW[7]. Alternatively, a highly active Dsr complex may be crucial for the removal of toxic sulfite to prevent inhibition of the sensitive Mcr complex. Moreover, the Dsr complex together with hydrogenases provide a capacity for non-methanogenic growth by means of sulfite reduction coupled to hydrogen oxidation; however, our attempts to sustain culture LCB3 on sulfite and hydrogen were unsuccessful.

Conclusion

Here, we demonstrate that methanogenesis is not restricted to the Euryarchaeota superphylum by culturing '*Ca*. M. washburnensis' strain LCB3, a methanogenic representative of the Korarchaeia from a terrestrial hot spring. During growth, strain LCB3 forms methane from methanol, shows translational activity reliant on the function of the MCR complex and expresses genes involved in energy conservation by means of methanogenesis. The confirmation that a member of the deepest branching lineage within the Thermoproteota superphylum is a methanogen has important implications for our understanding of the evolution and diversification of methanogens. Notably, growth of strain LCB3 at 77 °C extends the upper temperature range of both methyl-reducing and b-type cytochrome-involving methanogenesis. This may affect its niche differentiation, because cytochrome-based energy conservation is more efficient[15], however, no such methanogen has yet been studied in this regard. Strain LCB3 appears to be specialized towards using methanol as substrate for methanogenesis and incapable of exploiting methylated amines. However, strain LCB3 highly expressed a diverse set of energy-conserving complexes and the potential to use electron donors other than hydrogen, which is rare in cultured methyl-reducing methanogens[12,22]. Our genomic, transcriptomic and growth experimental evaluation of strain LCB3 indicated metabolic traits unique among methanogens and suggests that many yet unresolved aspects of its physiology, biochemistry, cell biology and ecology await discovery.

So far, '*Ca*. M. washburnensis' LCB3 is the second member of the Korarchaeia obtained in an enrichment culture and it contrasts the non-methanogenic peptide fermenter '*Ca*. K. cryptofilum'[23]. Cultivation of '*Ca*. M. washburnensis' opens the possibility for fundamental research on the evolution and biology of Korarchaeia and to expand our understanding of methanogenesis and the transition between methanogenic and non-methanogenic lifestyles.

Online content

Any methods, additional references, Nature Portfolio reporting summaries, source data, extended data, supplementary information, acknowledgements, peer review information; details of author contributions and competing interests; and statements of data and code availability are available at https://doi.org/10.1038/s41586-024-07829-8.

1. Seitz, K. W. et al. Asgard archaea capable of anaerobic hydrocarbon cycling. *Nat. Commun.* **10**, 1822 (2019).
2. Evans, P. et al. Methane metabolism in the archaeal phylum Bathyarchaeota revealed by genome-centric metagenomics. *Science* **350**, 434–438 (2015).
3. Vanwonterghem, I. et al. Methylotrophic methanogenesis discovered in the archaeal phylum Verstraetearchaeota. *Nat. Microbiol.* **1**, 16170 (2016).
4. Hua, Z. S. et al. Insights into the ecological roles and evolution of methyl-coenzyme M reductase-containing hot spring Archaea. *Nat. Commun.* **10**, 4574 (2019).
5. Borrel, G. et al. Wide diversity of methane and short-chain alkane metabolisms in uncultured archaea. *Nat. Microbiol.* **4**, 603–613 (2019).

6. Wang, Y., Wegener, G., Hou, J., Wang, F. & Xiao, X. Expanding anaerobic alkane metabolism in the domain of Archaea. *Nat. Microbiol.* **4**, 595–602 (2019).
7. McKay, L. J. et al. Co-occurring genomic capacity for anaerobic methane and dissimilatory sulfur metabolisms discovered in the Korarchaeota. *Nat. Microbiol.* **4**, 614–622 (2019).
8. Saunois, M. et al. The global methane budget 2000-2017. *Earth Syst. Sci. Data* **12**, 1561–1623 (2020).
9. Conrad, R. The global methane cycle: recent advances in understanding the microbial processes involved. *Environ. Microbiol. Rep* **1**, 285–292 (2009).
10. Garcia, P. S., Gribaldo, S. & Borrel, G. Diversity and evolution of methane-related pathways in Archaea. *Annu. Rev. Microbiol.* **76**, 727–755 (2022).
11. Enzmann, F., Mayer, F., Rother, M. & Holtmann, D. Methanogens: biochemical background and biotechnological applications. *AMB Express* **8**, 2–22 (2018).
12. Kurth, J. M., Huub, Op Den Camp, J. M. & Welte, C. U. Several ways one goal-methanogenesis from unconventional substrates. *Appl. Microbiol. Biotechnol.* **104**, 6839–6854 (2020).
13. Thauer, R. K. Methyl (alkyl)-coenzyme M reductases: nickel F-430-containing enzymes Involved in anaerobic methane formation and in anaerobic oxidation of methane or of short chain alkanes. *Biochemistry* **58**, 5198–5220 (2019).
14. Scheller, S., Goenrich, M., Boecher, R., Thauer, R. K. & Jaun, B. The key nickel enzyme of methanogenesis catalyses the anaerobic oxidation of methane. *Nature* **465**, 606–608 (2010).
15. Thauer, R. K., Kaster, A. K., Seedorf, H., Buckel, W. & Hedderich, R. Methanogenic archaea: ecologically relevant differences in energy conservation. *Nat. Rev. Microbiol.* **6**, 579–591 (2008).
16. Oren, A. & Garrity, G. M. Candidatus list no. 2. lists of names of prokaryotic candidatus taxa. *Int. J. Syst. Evol. Microbiol.* https://doi.org/10.1099/ijsem.0.004671 (2021).
17. Lynes, M. M. et al. Diversity and function of methyl-coenzyme M reductase-encoding archaea in Yellowstone hot springs revealed by metagenomics and mesocosm experiments. *ISME Comm.* **3**, 22 (2023).
18. McKay, L. J., Hatzenpichler, R., Inskeep, W. P. & Fields, M. W. Occurrence and expression of novel methyl-coenzyme M reductase gene (mcrA) variants in hot spring sediments. *Sci. Rep.* **7**, 7252 (2017).
19. Zeikus, J. G., Ben-Bassat, A. & Hegge, P. W. Microbiology of methanogenesis in thermal, volcanic envirorunments. *J. Bacteriol.* **143**, 432–440 (1980).
20. McKay, L. J., Klingelsmith, K. B., Deutschbauer, A. M., Inskeep, W. P. & Fields, M. W. Draft genome sequence of *Methanothermobacter thermautotrophicus* WHS, a thermophilic hydrogenotrophic methanogen from Washburn Hot Springs in Yellowstone National Park, USA. *Microbiol. Resour. Announc.* **10**, e01157-20 (2021).
21. Cheng, L. et al. *Methermicoccus shengliensis* gen. nov., sp. nov., a thermophilic, methylotrophc methanogen isolated from oil-production water, and proposal of *Methermicoccaceae* fam. nov. *Int. J. Syst. Evol. Microbiol.* **57**, 2964–2969 (2007).
22. Sorokin, Di. Y. et al. Discovery of extremely halophilic, methyl-reducing euryarchaea provides insights into the evolutionary origin of methanogenesis. *Nat. Microbiol.* **2**, 17081 (2017).
23. Elkins, J. G. et al. A korarchaeal genome reveals insights into the evolution of the Archaea. *Proc. Natl Acad. Sci. USA* **105**, 8102–8107 (2008).
24. Søndergaard, D., Pedersen, C. N. S. & Greening, C. HydDB: a web tool for hydrogenase classification and analysis. *Sci Rep.* **6**, 34212 (2016).
25. Calisto, F. & Pereira, M. M. The ion-translocating NrfD-like subunit of energy-transducing membrane complexes. *Front. Chem.* **9**, 663706 (2021).
26. Ogawa, T., Yoshimura, T. & Hemmi, H. Geranylfarnesyl diphosphate synthase from *Methanosarcina mazei*: different role, different evolution. *Biochem. Biophys. Res. Commun.* **393**, 16–20 (2010).
27. Ellenbogen, J. B., Jiang, R., Kountz, D. J., Zhang, L. & Krzycki, J. A. The MttB superfamily member MtyB from the human gut symbiont *Eubacterium limosum* is a cobalamin-dependent γ-butyrobetaine methyltransferase. *J. Biol. Chem.* **297**, 101327 (2021).
28. Ticak, T., Kountz, D. J., Girosky, K. E., Krzycki, J. A. & Ferguson, D. J. Jr A nonpyrrolysine member of the widely distributed trimethylamine methyltransferase family is a glycine betaine methyltransferase. *Proc. Natl Acad. Sci. USA* **111**, E4668–E4676 (2014).
29. Kountz, D. J., Behrman, E. J., Zhang, L. & Krzycki, J. A. MtcB, a member of the MttB superfamily from the human gut acetogen *Eubacterium limosum*, is a cobalamin-dependent carnitine demethylase. *J. Biol. Chem.* **295**, 11971–11981 (2020).
30. Kulkarni, G., Mand, T. D. & Metcalf, W. W. Energy conservation via hydrogen cycling in the methanogenic archaeon *Methanosarcina barkeri*. *mBio.* **9**, e01256-18 (2018).
31. Schut, G. J., Lipscomb, G. L., Nguyen, D. M. N., Kelly, R. M. & Adams, M. W. W. Heterologous production of an energy-conserving carbon monoxide dehydrogenase complex in the hyperthermophile *Pyrococcus furiosus*. *Front. Microbiol.* **7**, 29 (2016).
32. Kim, M. S. et al. Co-dependent H_2 production by genetically engineered *Thermococcus onnurineus* NA1. *Appl. Environ. Microbiol.* **79**, 2048–2053 (2013).
33. Kim, M. S. et al. A novel co-responsive transcriptional regulator and enhanced H_2 production by an engineered *Thermococcus onnurineus* NA1 strain. *Appl. Environ. Microbiol.* **81**, 1708–1714 (2015).

Methods

Chemicals

All chemicals were purchased from Sigma Aldrich unless otherwise specified.

Sample collection, enrichment and cultivation

Hot spring sediment was retrieved from three geothermal features in YNP: LCB003 (44.57763, −110.78957; November 2020; 77 °C; pH 6.5), LCB058 (44.57039, −110.80521; October 2020; 70 °C; pH 6.1) located in the LCB and WHS (44.76493, −110.43030; October 2019; 64 °C; pH 6.4) thermal areas. A mixture of surface sediments (roughly 1 cm deep) and spring water were collected into glass bottles sealed headspace-free with a butyl rubber stopper. Slurries were stored at in situ temperature for 24 h before transfer to room temperature for long-term storage. Initial enrichments were initiated within 24 h of material retrieval from LCB003 and LCB058 or within 2 years of material retrieval from WHS, and were set up in sterile serum vials (50 or 70 ml) under a N_2–CO_2–H_2 (90/5/5%) atmosphere. Slurries from LCB058 and WHS were diluted with anoxic medium (1:10). Medium was prepared as described previously[34] and contained KH_2PO_4, 0.5 g l^{-1}; $MgSO_4 \cdot 7H_2O$, 0.4 g l^{-1}; NaCl, 0.5 g l^{-1}; NH_4Cl, 0.4 g l^{-1}; $CaCl_2 \cdot 2H_2O$, 0.05 g l^{-1}; MES, 2.17 g l^{-1}; yeast extract, 0.1 g l^{-1} and 0.002% (w/v) $(NH_4)_2Fe(SO_4)_2 \cdot 6H_2O$, 5 mM $NaHCO_3$, 1 ml l^{-1} trace element solution SL-10, 1 ml l^{-1} selenite-tungstate solution[35], 1 ml l^{-1} CCM vitamins[36], 0.0005% (w/v) resazurin, 10 ml g l^{-1} of coenzyme M, 2 ml l^{-1} sodium dithionite, 1 mM dithiothreitol and 1 mM $Na_2S \cdot 9H_2O$, with pH adjusted to 6.5 with NaOH. Serum vials were sealed with butyl rubber stoppers and aluminium crimps before the headspace was degassed with N_2–CO_2 (90/10) for 5 min and set to 200 kPa. Hydrogen and methanol were added at final concentrations of 50% and 10 mM, respectively. Two types of incubation were prepared from the slurry of each hot spring. One was amended with the bacterial antibiotics streptomycin (50 mg l^{-1}; inhibitor of protein synthesis) and vancomycin (50 mg l^{-1}; inhibitor of peptidoglycan synthesis) and one was not amended with antibiotics. Further control incubations were supplied with only methanol or only hydrogen. Incubation was conducted at in situ temperatures. All stock solutions were anoxic and sterilized by filtration or autoclavation. After 64 days of incubation an initial enrichment from LCB003 (LCB003-1B) was selected as inoculum for the cultivation of '*Ca*. M. washburnensis' and transferred into anoxic medium (10% v/v), amended with hydrogen, methanol and antibiotics. Cultivation was conducted at 77 °C and cultures were maintained by regular transfer into fresh medium (10% v/v).

Methane measurements

Methane concentrations were determined from subsamples of 250 µl of headspace gas collected with a gas tight syringe (Hamilton) and injected into 10 ml autosampler vials sealed with grey chlorobutyl septa. Subsamples were injected with a robotic autosampler (AOC-6000) into a Shimadzu 2020-GC equipped with a GS-CarbonPLOT column (30 m × 0.32 mm; 1.5 µm film thickness; Agilent) and a Rt-Q-BOND column (30 × 0.32 mm; 1.5 µm film thickness; Restek) and operated with injector, column and flame ionization detector maintained at 200, 50 and 240 °C, respectively. Methane concentrations were calculated on the basis of injection of a standard curve. Data were analysed using the Shimadzu LabSolutions software.

Stable isotope incubation

For tracking the conversion of ^{13}C-methanol to ^{13}C-methane, active enrichment cultures were incubated in the presence of ^{13}C-methanol (99% labelled; Cambridge Isotope Laboratories). Here, 30 ml incubations were carried out in 60 ml serum bottles with 20% (v/v) inoculum. Control incubations were performed in the presence of (1) ^{12}C-methanol (100%), (2) ^{13}C-methanol (100%) plus BES to inhibit methanogenesis, (3) ^{13}C-methanol (100%) plus paraformaldehyde (PFA) to inhibit cellular activity and (4) ^{13}C-methanol (100%) without inoculum. Substrate and inhibitor were added at a concentration of 10 mM. Headspace samples were collected regularly as described above and analysed using a Shimadzu QP2020 NX GCMS equipped with a GS-CarbonPLOT column (30 m × 0.35 mm; 30 µm film thickness; Agilent) and operated in Selected Ion Monitoring mode. The instrument was operated as previously described[37]. Peak areas corresponding to m/z ratios of 16 for ^{12}C-methane, 17 for ^{13}C-methane were used for quantification.

FISH and cell counts

Aliquots of enrichment cultures were fixed in 2% PFA for 1 h at room temperature, washed twice by centrifugation at 16,000*g*, removing the supernatant and resuspending the cells in 1× PBS, before cell suspensions were stored at 4 °C. For direct cell counts, aliquots of fixed cell suspensions were filtered onto polycarbonate filters (0.2 µm pore size, 25 mm diameter, GTTP Millipore) and air dried before filter pieces were cut, stained with DAPI (4,6-diamidino-2-phenylindole), embedded in Citifluor-Vectashield and enumerated under an epifluorescence microscope (Leica DM4B). Relative abundance of target cells was determined from the fraction of CARD-FISH or DOPE-FISH stained cells compared to total cell counts on the basis of DNA stained cells using DAPI. A 16S rRNA-targeted oligonucleotide probe (KRmw515, 5′-CCA GCC TTG CCC TCC CCT-3′) specific for '*Ca*. M. washburnensis' was designed using the probe design tool in the ARB software package[38] and tested in silico using TestProbe (https://www.arb-silva.de/search/testprobe/). Probe KRmw515 has one mismatch to the 16S rRNA of non-target organism '*Ca*. K. cryptofilum', which was absent from the culture. The horseradish peroxidase (HRP)-labelled oligonucleotide probe was synthesized by Biomers. Stringency was tested in a CARD-FISH experiment by increasing the formamide concentration in the hybridization buffer from 0 to 70%. CARD-FISH was performed as described previously[39]. Cell wall permeabilization was achieved with lysozyme treatment for 30 min at 37 °C (10 mg ml^{-1} lysozyme, lyophilized powder in 0.1 M Tris-HCl, 0.05 M EDTA, pH 8) followed by proteinase K digestion for 10 min at room temperature (4.5 mU ml^{-1} proteinase K (Merck) in 0.1 M Tris-HCl, 0.05 M EDTA and 0.5 M NaCl, pH 8). Endogenous peroxidases were inactivated with 0.15% H_2O_2 in methanol (30 min, room temperature). For hybridization, the following oligonucleotide probes were applied at a concentration of 35% formamide: EUB338I-III (ref. 40), Arch915 (ref. 41), NON338 (ref. 42) and KRmw515. CARD was performed using tyramides labelled with the fluorochromes Alexa Fluor 594 or Alexa Fluor 488. When performing double hybridizations, the peroxidase enzymes of the first hybridization were inactivated with 0.3% H_2O_2 in methanol (30 min, room temperature) before hybridization with the second HRP-labelled probe. DOPE-FISH was performed as previously described[43]. Samples were stained with DAPI, embedded in Citifluor-Vectashield and visualized using epifluorescence microscopy; images were acquired using LeicaX software and analysed using Fiji (https://github.com/fiji/fiji).

BONCAT-FISH experiments

The metabolic activity of strain LCB3 under methanogenic versus methanogenesis-inhibited conditions was tested using BONCAT. Replicate incubations of culture LCB3 were initiated with methanol and hydrogen. Inhibited controls were amended with BES at day 0. When methane production reached exponential phase (day 15), triplicate cultures were either amended with BES (5 mM) or remained unamended. After 72 h both sets were spiked with the bioorthogonal amino acid HPG (100 µM). Subsamples were retrieved after 24 h, fixed in 2% PFA, washed and stored in 1× PBS at 4 °C. Aliquots of fixed samples were spotted on glass slides and BONCAT-FISH was performed as previously described[44]. The fractions of BONCAT-labelled, FISH-labelled and DAPI-stained cells were enumerated to determine the relative abundance of BONCAT and FISH-labelled cells using Fiji (https://github.com/fiji/fiji).

Growth experiments

To test whether substrates other than methanol support methanogenic growth 10 mM of monomethylamine, dimethylamine, trimethylamine, ethanol or 2-propanol were added to culture LCB3 in the presence of hydrogen (50%). Furthermore, culture LCB3 was supplemented with 2 mM L-lactate plus MeOH (10 mM) or plus MeOH (10 mM) and hydrogen (50%). Methane production was monitored over an incubation time of 85 days.

Amplicon sequencing and analysis

DNA was extracted from environmental samples, and from initial enrichment cultures (pellet from 0.5 ml) using the FastDNA Spin Kit for Soil (MP Biomedicals) following the manufacturer's guidelines. *mcrA* genes were amplified with primer set mlas-mod-F/mcrA-rev-R[45,46], and archaeal and bacterial 16S rRNA genes were amplified with the updated Earth Microbiome Project primer set 515F and 806R[47–49]. Amplicon libraries were prepared as previously described[50] and sequenced at the Molecular Research Core Facility at Idaho State University (Pocatello, ID, USA) using an Illumina MiSeq platform with 2 × 300 basepair (bp) (*mcrA* amplicon library) and 2 × 250 bp (16S rRNA amplicon library) paired-end read chemistry. Both 16S rRNA and *mcrA* gene reads were processed using QIIME 2 v.2020.2 (ref. 51) Primer sequences were removed from demultiplexed reads using cutadapt[52] with error rate 0.12, and reads were truncated (145 bp forward, 145 bp reverse and 260 bp forward, 200 bp reverse for 16S rRNA and *mcrA* datasets, respectively), filtered, denoised and merged in DADA2 with default settings[53]. 16S rRNA gene amplicon sequence variants (ASVs) were taxonomically classified with the sklearn method and the SILVA 132 database[54]. *mcrA* gene ASVs were assigned a taxonomy using vsearch with a minimum identity of 70% and no consensus classification against a reference database of representative near-full length *mcrA* genes encompassing the diversity of publicly available *mcrA*. Contaminants were removed using the R package decontam[55]. The *mcrA* gene dataset was curated by removing ASVs less than or equal to 400 bp and non-*mcrA* gene ASVs as identified by evaluating the top hits of a blastx search against the National Center for Biotechnology Information (NCBI) NR database.

Metagenome sequencing

A 50 ml aliquot of culture LCB3 was centrifuged at 16,000*g* for 10 min to pellet cells, supernatant was removed, and the pellet stored at −80 °C. Genomic DNA was extracted from the pellet following a published protocol[56], with the following modifications: (1) cells were disrupted with a tissue grinder (Wheaton), (2) proteinase K treatment was extended to 1 h, and (3) DNA was precipitated in the presence of 0.7× volumes of isopropanol and 0.1× volume of 3 M sodium acetate. DNA extracts were purified using the Zymo clean and concentrator kit (DCC-10, Zymo Research) according to the manufacturer's instructions. Purified genomic DNA was used for metagenomic library construction with the Illumina DNA Prep kit following the manufacturer's recommendations and was sequenced on an Illumina NextSeq 2000 platform with 2 × 151 bp paired-end read chemistry performed at SeqCenter (Pittsburgh, PA, USA). Furthermore, for PacBio long-read sequencing a library was generated with a 6–10 kb ultra-low input kit and sequenced on a Sequel IIe platform at the Joint Genome Institute (Berkeley, CA, USA).

Metagenome assembly, binning and quality assessment

PacBio HiFi sequences were assembled with hifiasm-meta (v.0.3-r063.2; --force-rs)[57] that resulted in the recovery of complete circularized genomes of '*Ca*. M. washburnensis' and the other archaeal populations in culture LCB3 (Thermofilum, Archaeoglobaceae, Ignisphaera, Desulfurococcaeae and Fervidicoccaceae). The Thermofilum population was separated into two strains, one circularized and one near-complete linear contig. Genome completeness and redundancy were assessed using CheckM1 v.1.1.3 (ref. 58) and CheckM2 v.1.02 (ref. 59). Average nucleotide identity (ANI) and average amino acid identity (AAI) values were computed with CompareM v.0.0.23 (--fragLen 2000) (https://github.com/dparks1134/CompareM) and pyani v.0.2.12 (ANIb)[60], respectively, for available genomes and MAGs of '*Ca*. M. washburnensis' ($n = 4$) and selected '*Ca*. Korarchaeum' ($n = 2$) reference genomes.

Illumina read quality, linker and adaptor trimming, artefact and common contaminate removal and error correction were performed using the rqcfilter2 pipeline (maxns=3, maq=3) and bbcms (mincount=2, hcf=0.6) from the BBTools suite v.38.94 (Bushnell B. 2014. BBMap: a fast, accurate, splice-aware aligner. https://sourceforge.net/projects/bbmap). Resulting reads were assembled with SPAdes[61] v.3.15.3 (-k 33,55,77,99,127 –meta –only-assembler). Relative abundances were estimated by mapping the quality controlled Illumina reads to the PacBio assemblies with bbmap (ambiguous=random). Furthermore, the genome of strain LCB3 was used to recruit reads from various short-read metagenomes with bbmap (ambiguous=random) to determine the relative abundance of strain LCB3 in different geothermal features of YNP.

RNA extraction, sequencing and analysis

Six replicate cultures (75 ml each) were grown with methanol plus hydrogen to log phase of methane production. Culture bottles were rapidly cooled from 77 °C in a dry ice-ethanol bath (1 min) and kept on ice. Cells were concentrated onto sterivex filters that were then soaked in Zymo DNA/RNA Shield and immediately processed. The filters were placed into Zymo BashingBead lysis tubes (Zymo Research) containing 800 µl of Zymo RNA lysis buffer and vortexed at maximum speed for 20 min. The tubes were centrifuged at 14,000*g* for 15 min and the supernatant was used for RNA purification with the Zymo Quick-RNA miniprep kit according to the manufacturer's instructions and including the DNase I step. Owing to low biomass, the RNA from all six replicates was pooled and concentrated using the Zymo RNA Clean & Concentrator kit according to the manufacturer's instructions. Purified RNA was used for library preparation and sequencing at SeqCenter (Pittsburgh, PA, USA). RNA was treated again with DNase I (Invitrogen) before library preparation with Illumina's Stranded Total RNA Prep Ligation with Ribo-Zero Plus kit and 10 bp unique dual indices. Libraries were sequenced on a NovaSeq X Plus platform producing 2 × 150 bp reads. Demultiplexing, quality control and adaptor trimming was performed with bcl-convert (v.4.1.5). Reads were further processed with rqcfilter2 (rna=t, trimrnaadapter=t, qtrim=rl, trimq=10, maq=20, maxns=0, minlen=50, mlf=0.33, removeribo=f) and mapped to reference genomes from the LCB3 culture using bbmap (ambig=random). Reads mapping to rRNA genes were excluded before normalization. Reads mapping to each gene were normalized to gene length before calculating the centre log ratio ($\log_{10}$) and transcripts per kilobase million.

Annotation and reconstruction of metabolic potential

The genome of strain LCB3 was annotated by the IMG/M database[62]. Catalytic subunits of [NiFe] hydrogenases (PF00374) were initially classified with HydDB, checked for conserved CXXC motifs at the N and C terminus, and further classified by phylogenetic analyses[24]. Proteins encoded in the genome were assessed to identify c-type cytochromes as previously described[63]. Protein sequences were searched for CXXCH motifs, SignalP v.6.0 (ref. 64) was used to predict signal peptides and DeepTMHMM[65] was used to predict transmembrane helices. Eleven proteins contained one CXXCH motif but no transmembrane helices or signal peptides, indicating that they are not c-type cytochromes. Genes encoding proteins necessary for the biosynthesis of c-type cytochromes (Ccm machinery) were not identified in the LCB3 genome. Predicted optimal growth temperatures of MAGs and genomes were determined with Tome predOGT[66].

Phylogenetic analyses and distribution of marker genes

A set of 33 single-copy marker proteins was collected from Korarchaeia MAGs and reference archaeal genomes. These markers were aligned with MUSCLE[67], trimmed with trimAL[68] using a 50% gap threshold and concatenated to produce a final alignment of 7,118 positions. Iqtree2 (ref. 69) was used to reconstruct a maximum-likelihood phylogenetic tree, using the LG+F+R10 model, 1,000 ultrafast bootstraps and 1,000 iterations of the SH-like approximate-likelihood ratio test[70].

16S rRNA genes from the metagenome of culture LCB3 and references were aligned and masked with ssu-align, and a maximum-likelihood phylogenetic tree was constructed with fasttree[71]. McrA from the genome of strain LCB3 and publicly available references were aligned with MAFFT-linsi[72], trimmed with trimAL[68] with 50% gap threshold and used for maximum-likelihood phylogenetic analysis with Iqtree2 (ref. 69) with LG+C60+F+G model and 1,000 ultrafast bootstraps.

Catalytic subunits of group 1 and group 4 [NiFe]-hydrogenases were extracted from the genome of strain LCB3 aligned against HydDB[24] reference sequences with Mafft-LINSi[72] and trimmed with trimAL[68] using a 50% gap threshold. For group 4, additional sequences of subunits FpoD/NuoD belonging to respiratory complexes were collected from Ou et al.[73] and included in the alignments. This produced final alignments of 562 and 365 residues for group 1 and group 4, respectively. Maximum-likelihood phylogenetic trees were constructed using Iqtree2 (ref. 69) with best-fit model selected according to Bayesian information criterion and 1,000 ultrafast bootstraps. The models used were LG+R10 for group 1 and LG+C60+R+F for group 4.

Geranylfarnesyl diphosphate synthase homologues were collected by searching for COG0142 and further classified by phylogenetic analysis in comparison with sequences identified in other studies[26,73]. Sequences were aligned with Mafft-LINSi and trimmed with trimal using a 50% gap threshold, producing a final alignment of 327 residues. A maximum-likelihood phylogenetic tree was constructed using Iqtree2 with a best-fit model LG+I+G4 selected according to Bayesian information criterion and 1,000 ultrafast bootstraps.

The environmental distribution of '*Ca*. M. washburnensis' was assessed through the IMNGS webserver[74] on 20 October 2023. The 16S rRNA gene of strain LCB3 was used to search the NCBI Sequence Read Archive with a similarity cutoff of 99 or 97% and a minimum size of 200 bp. The 16S rRNA gene and McrA of strain LCB3 were also used to search assembled metagenomes available on the JGI IMG/MER webserver (n = 12,114 on 7 November 2023) with blastn and blastp, respectively.

Etymology. *Methanodesulfokora*, *methanum* (Latin): methane, *de* (Latin): from, *sulfo* (Latin): sulfur, *kore* (Greek): young woman; *washburnensis* (Latin): pertaining to Washburn Hot Springs. The name implies a methane and sulfur metabolizing member of the class Korarchaeia within the phylum Thermoproteota, which MAG was first obtained from Washburn Hot Springs in YNP[7]. The archaeon cultured in this study represents '*Ca*. M. washburnensis' strain LCB3.

Locality. Enriched from geothermally heated sediment of an unnamed hot spring, catalogued as feature LCB003 (ref. 17), in the LCB of YNP, WY, USA.

Diagnosis. Anaerobic, thermophilic, methyl-reducing methanogen of filamentous morphology.

Reporting summary

Further information on research design is available in the Nature Portfolio Reporting Summary linked to this article.

Data availability

The 16S rRNA gene and *mcrA* gene amplicon data, metagenomic reads and metatranscriptomic reads are deposited at NCBI under BioProject PRJNA913929. Metagenomes and genomes are available on IMG/M (JGI) under IMG Genome IDs 3300005860 (WHS), 3300043541 (LCB058), 3300028675 (LCB003), 8012931703 ('*Ca*. M. washburnensis' strain LCB3), 8015587805 (Archaeoglobaceae archaeon LCB3), 8015589684 (*Thermofilum* sp. LCB3-A), 8015591669 (*Thermofilum* sp. LCB3-B), 8015593670 (Fervidicoccaceae archaeon LCB3), 8015596852 (*Ignisphaera* sp. LCB3) and 8015595177 (Desulfurococcaceae archaeon LCB3). Source data are provided with this paper.

34. Laso-Pérez, R., Krukenberg, V., Musat, F. & Wegener, G. Establishing anaerobic hydrocarbon-degrading enrichment cultures of microorganisms under strictly anoxic conditions. *Nat. Protoc.* **13**, 1310–1330 (2018).
35. Friedrich Widdel, F. B. Gram-negative mesophilic sulfate-reducing bacteria. *Prokaryotes* **4**, 3352–3378 (1992).
36. Brandis, A. & Thauer, R. K. Growth of *Desulfurovibrio* species on hydrogen and sulphate as sole energy source. *J. Gen. Microbiol.* **126**, 249–252 (1981).
37. Ai, G., Zhu, J., Dong, X. & Sun, T. Simultaneous characterization of methane and carbon dioxide produced by cultured methanogens using gas chromatography/isotope ratio mass spectrometry and gas chromatography/mass spectrometry. *Rapid Commun. Mass Spectrom.* **27**, 1935–1944 (2013).
38. Ludwig, W. et al. ARB: a software environment for sequence data. *Nucleic Acids Res.* **32**, 1363–1371 (2004).
39. Pernthaler, A., Pernthaler, J. & Amann, R. Fluorescence in situ hybridization and catalyzed reporter deposition for the identification of marine bacteria. *Appl. Environ. Microbiol.* **68**, 3094–3101 (2002).
40. Daims, H., Bruhl, A., Amann, R., Schleifer, K. & Wagner, M. The domain-specific probe EUB338 is insufficient for the detection of all Bacteria: development and evaluation of a more comprehensive probe set. *Syst. Appl. Microbiol.* **22**, 434–444 (1999).
41. Stahl, D. A. & Amann, R. in *Nucleic Acid Techniques in Bacterial Systematics* (eds Stackebrandt, E. & Goodfellow, M.) 205–248 (Wiley, 1991).
42. Wallner, G., Amann, R. & Beisker, W. Optimizing fluorescent in situ hybridization with rRNA-targeted oligonucleotide probes for flow cytometric identification of microorganisms. *Cytometry* **14**, 136–143 (1993).
43. Stoecker, K., Dorninger, C., Daims, H. & Wagner, M. Double labeling of oligonucleotide probes for fluorescence in situ hybridization (DOPE-FISH) improves signal intensity and increases rRNA accessibility. *Appl. Environ. Microbiol.* **76**, 922–926 (2010).
44. Hatzenpichler, R. et al. Visualizing in situ translational activity for identifying and sorting slow-growing archaeal–bacterial consortia. *Proc. Natl Acad. Sci. USA* **113**, 4069–4078 (2016).
45. Steinberg, L. M. & Regan, J. M. mcrA-targeted real-time quantitative PCR method to examine methanogen communities. *Appl. Environ. Microbiol.* **75**, 4435–4442 (2009).
46. Angel, R., Claus, P. & Conrad, R. Methanogenic archaea are globally ubiquitous in aerated soils and become active under wet anoxic conditions. *ISME J.* **6**, 847–862 (2012).
47. Parada, A. E., Needham, D. M. & Fuhrman, J. A. Every base matters: assessing small subunit rRNA primers for marine microbiomes with mock communities, time series and global field samples. *Environ. Microbiol.* **18**, 1403–1414 (2016).
48. Apprill, A., Mcnally, S., Parsons, R. & Weber, L. Minor revision to V4 region SSU rRNA 806R gene primer greatly increases detection of SAR11 bacterioplankton. *Aquat. Microb. Ecol.* **75**, 129–137 (2015).
49. Thompson, L. R. et al. A communal catalogue reveals Earth's multiscale microbial diversity. *Nature* **551**, 457–463 (2017).
50. Krukenberg, V., Reichart, N. J., Spietz, R. L. & Hatzenpichler, R. Microbial community response to polysaccharide amendment in anoxic hydrothermal sediments of the Guaymas Basin. *Front. Microbiol.* **12**, 763971 (2021).
51. Bolyen, E. et al. Reproducible, interactive, scalable and extensible microbiome data science using QIIME 2. *Nat. Biotechnol.* **37**, 852–857 (2019).
52. Martin, M. Cutadapt removes adapter sequences from high-throughput sequencing reads. *EMBnet J.* **17**, 10–12 (2011).
53. Callahan, B. J. et al. DADA2: High-resolution sample inference from Illumina amplicon data. *Nat. Methods* **13**, 581–583 (2016).
54. Quast, C. et al. The SILVA ribosomal RNA gene database project: improved data processing and web-based tools. *Nucleic Acids Res.* **41**, D590–D596 (2013).
55. Davis, N. M., Proctor, D. M., Holmes, S. P., Relman, D. A. & Callahan, B. J. Simple statistical identification and removal of contaminant sequences in marker-gene and metagenomics data. *Microbiome* **6**, 226 (2018).
56. Zhou, J., Bruns, M. A. & Tiedje, J. M. DNA recovery from soils of diverse composition. *Appl. Environ. Microbiol.* **62**, 316–322 (1996).
57. Feng, X., Cheng, H., Portik, D. & Li, H. Metagenome assembly of high-fidelity long reads with hifiasm-meta. *Nat. Methods* **19**, 671–674 (2022).
58. Parks, D. H., Imelfort, M., Skennerton, C. T., Hugenholtz, P. & Tyson, G. W. CheckM: assessing the quality of microbial genomes recovered from isolates, single cells, and metagenomes. *Genome Res.* **25**, 1043–1055 (2015).
59. Chklovki, A., Parks, D. H., Woodcroft, B. J. & Tyson, G. W. CheckM2: a rapid, scalable and accurate tool for assessing microbial genome quality using machine learning. *Nat. Methods* **20**, 1203–1212 (2023).
60. Prichard, L., Glover, R. H., Humphris, S., Elphinstone, J. G. & Toth, I. K. Genomics and taxonomy in diagnostics for food security: soft-rotting enterobacterial plant pathogens. *Anal. Methods* **8**, 12–24 (2016).

61. Nurk, S., Meleshko, D., Korobeynikov, A. & Pevzner, P. A. MetaSPAdes: a new versatile metagenomic assembler. *Genome Res.* **27**, 824–834 (2017).
62. Chen, I. M. A. et al. IMG/M v.5.0: an integrated data management and comparative analysis system for microbial genomes and microbiomes. *Nucleic Acids Res.* **47**, D666–D677 (2019).
63. Kletzin, A. et al. Cytochromes c in Archaea: distribution, maturation, cell architecture, and the special case of *Ignicoccus hospitalis*. *Front. Microbiol.* **6**, 439 (2015).
64. Teufel, F. et al. SignalP 6.0 predicts all five types of signal peptides using protein language models. *Nat. Biotechnol.* **40**, 1023–1025 (2022).
65. Hallgren, J. et al. DeepTMHMM predicts alpha and beta transmembrane proteins using deep neural networks. Preprint at *bioRxiv* https://doi.org/10.1101/2022.04.08.487609 (2022).
66. Li, G., Rabe, K. S., Nielsen, J. & Engqvist, M. K. M. Machine learning applied to predicting microorganism growth temperatures and enzyme catalytic optima. *ACS Synth. Biol.* **8**, 1411–1420 (2019).
67. Edgar, R. C. MUSCLE: multiple sequence alignment with high accuracy and high throughput. *Nucleic Acids Res.* **32**, 1792–1797 (2004).
68. Capella-Gutiérrez, S., Silla-Martínez, J. M. & Gabaldón, T. trimAl: a tool for automated alignment trimming in large-scale phylogenetic analyses. *Bioinformatics* **25**, 1972–1973 (2009).
69. Minh, B. Q. et al. IQ-TREE 2: new models and efficient methods for phylogenetic inference in the genomic era. *Mol. Biol. Evol.* **37**, 1530–1534 (2020).
70. Guindon, S. et al. New algorithms and methods to estimate maximum-likelihood phylogenies: assessing the performance of PhyML 3.0. *Syst. Biol.* **59**, 307–321 (2010).
71. Price, M. N., Dehal, P. S. & Arkin, A. P. Fasttree: computing large minimum evolution trees with profiles instead of a distance matrix. *Mol. Biol. Evol.* **26**, 1641–1650 (2009).
72. Katoh, K. & Standley, D. M. MAFFT multiple sequence alignment software version 7: Improvements in performance and usability. *Mol. Biol. Evol.* **30**, 772–780 (2013).
73. Ou, Y. F. et al. Expanding the phylogenetic distribution of cytochrome b-containing methanogenic archaea sheds light on the evolution of methanogenesis. *ISME J.* **16**, 2373–2387 (2022).
74. Lagkouvardos, I. et al. IMNGS: a comprehensive open resource of processed 16S rRNA microbial profiles for ecology and diversity studies. *Sci. Rep.* **6**, 33721 (2016).

Acknowledgements This study was funded through a NASA Exobiology programme award (grant no. 80NSSC19K1633). V.K. was supported in part by a grant from the NSF (grant no. MCB-1817428 to R.H.). A.K. was supported in part by a fellowship by the Montana Space Grant Consortium. A portion of this research was performed under the Facilities Integrating Collaborations for User Science programme (proposal no. 10.46936/fics.proj.2017.49972/6000002) and the Community Science Program (proposal no. 10.46936/10.25585/60008108), and used resources at the Department of the Environment (DOE) Joint Genome Institute (https://ror.org/04xm1d337), which is a DOE Office of Science User Facility operated under contract no. DE-AC02-05CH11231. We thank the US National Park Service for permitting work in YNP under permit number YELL-SCI-8010. We thank L. McKay and M. Lynes (both Montana State University) for discussions that informed field sampling, cultivation, taxonomy and manuscript preparation, S. Scheller (Aalto University) for discussing methanogen biochemistry and P. Schlegel (Montana State University) for assistance in cultivation.

Author contributions V.K., A.J.K. and R.H. designed experiments. V.K., A.J.K. and Z.J.J. conducted field work, reconstructed the metabolic potential of strain LCB3 and performed phylogenetic analysis. V.K. and A.J.K. performed cultivation and analysed gene expression data. Z.J.J. and A.J.K. processed metagenomic data and performed phylogenomic analysis. V.K. performed amplicon sequencing, BONCAT and CARD-FISH experiments. A.J.K. extracted DNA for metagenome sequencing, performed FISH, stable isotope tracing, substrate testing and transcriptomics experiments, and developed gas chromatography and mass spectrometry protocols. Z.J.J. performed whole-genome comparisons and determined environmental distributions. R.H. was responsible for funding and supervision of the project. All authors contributed to writing of the paper.

Competing interests The authors declare no competing interests.

Additional information

Supplementary information The online version contains supplementary material available at https://doi.org/10.1038/s41586-024-07829-8.

Correspondence and requests for materials should be addressed to Viola Krukenberg or Roland Hatzenpichler.

Peer review information *Nature* thanks Cornelia Welte and the other, anonymous, reviewer(s) for their contribution to the peer review of this work.

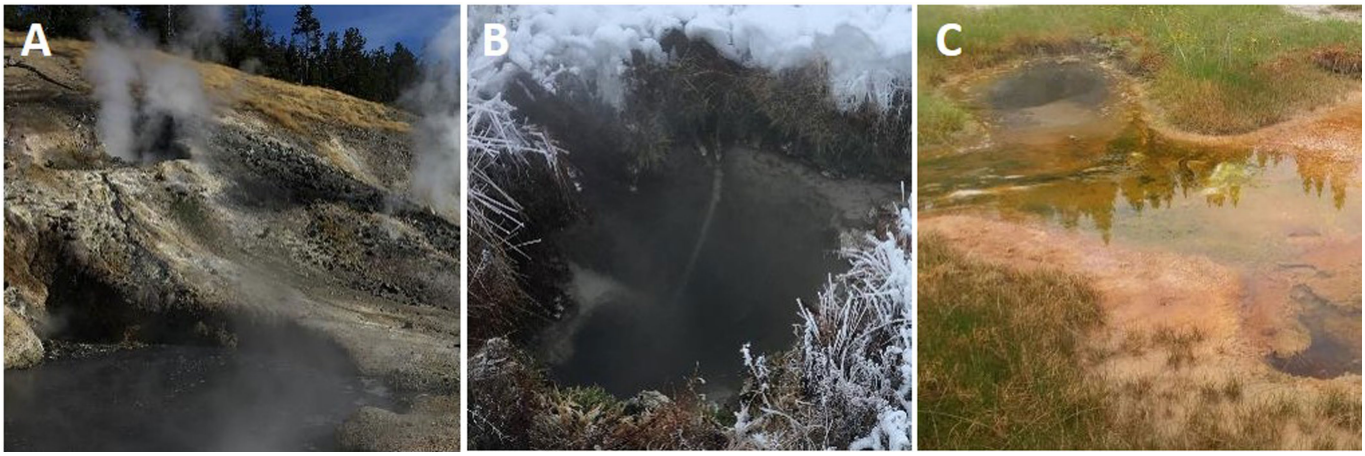

Extended Data Fig. 1 | Images of hot springs used as source material for cultivation. A. Washburn Hot Springs. **B**. Hot spring LCB003. **C**. Hot spring LCB058. All three hot springs are located in Yellowstone National Park (WY, USA).

All work in Yellowstone National Park was performed under research permit YELL-SCI-8010 to R.H.

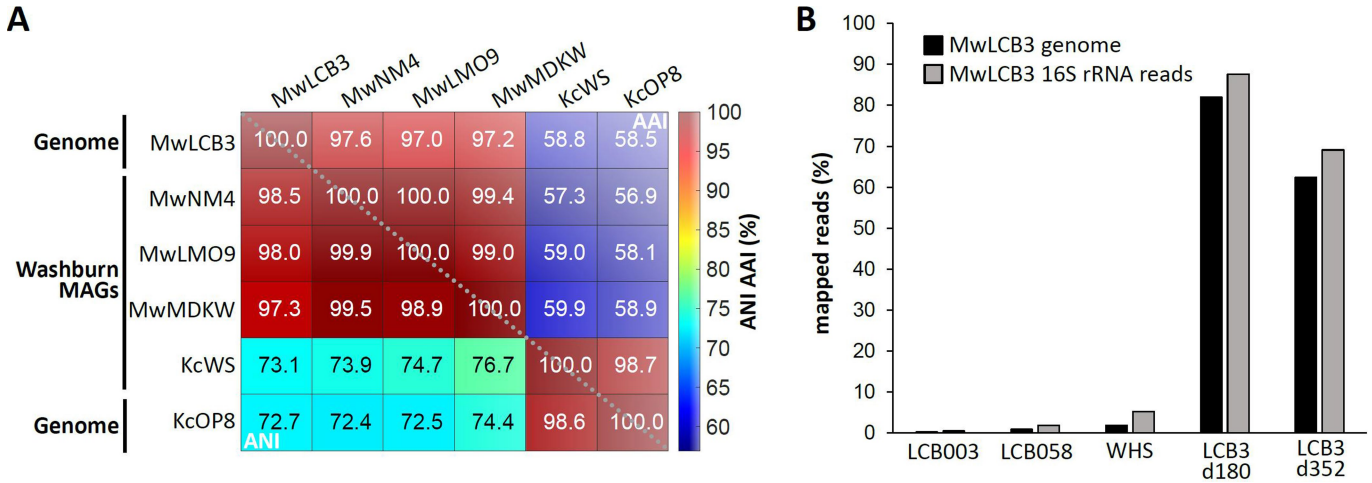

Extended Data Fig. 2 | Comparison of Korarchaeia genomes and MAGs. **A**. Pairwise comparisons of average nucleotide (below dotted line) and amino acid (above dotted line) identities (%) of '*Ca*. Methanodesulfokora' and '*Ca*. Korarchaeum' genomes and Washburn Hot Spring MAGs. **B**. '*Ca*. M. washburnensis' strain LCB3 genome and 16S rRNA gene read abundances in environmental metagenomes LCB003, LCB058, and WHS and in culture LCB3 at day 180 and 352.

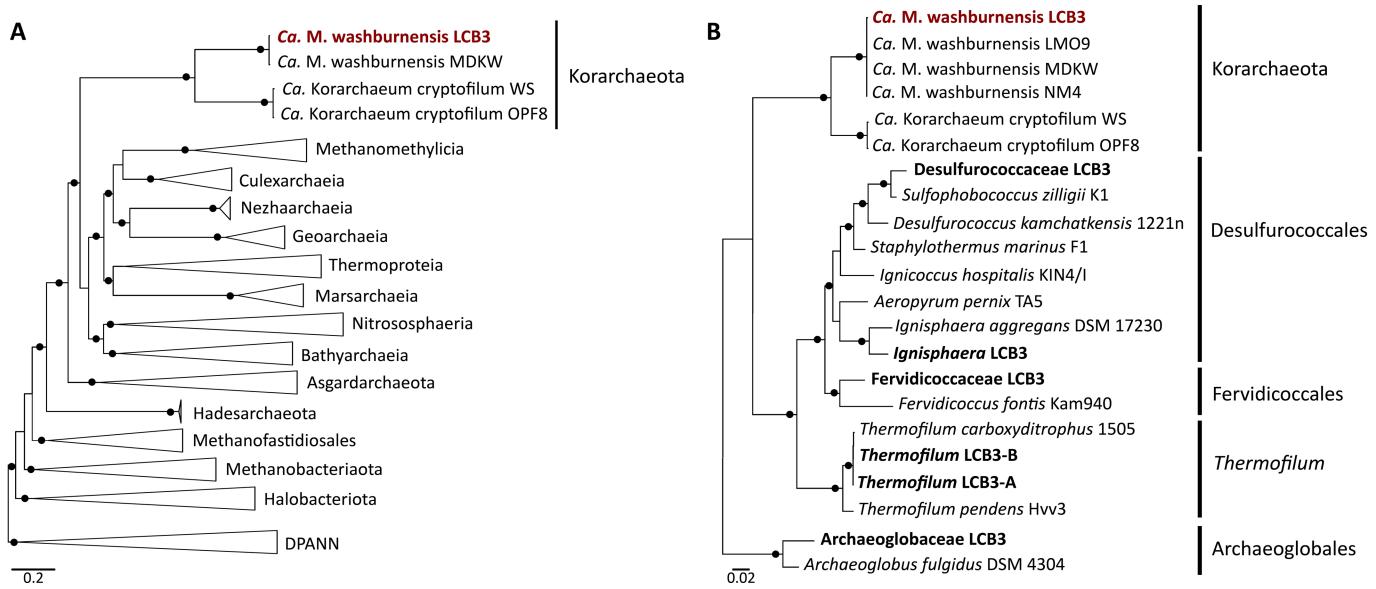

Extended Data Fig. 3 | Phylogenetic affiliation of '*Ca*. M. washburnensis' strain LCB3. A. Maximum likelihood phylogenomic tree of archaea based on 33 single copy marker genes. The tree was constructed with IQtree and the best-fit model LG+F+R10, from the concatenated alignment of conserved arCOGs. The '*Ca*. M. washburnensis' strain LCB3 genome is highlighted in red. Circles indicate ultrafast bootstrap values >95. **B**. Maximum likelihood phylogenetic tree of 16S rRNA genes from culture LCB3. The tree was constructed with fasttree including the 16S rRNA gene from the LCB3 genome (red), 16S rRNA genes in MAGs from culture LCB3 and reference sequences. Circles indicate bootstrap support values >95.

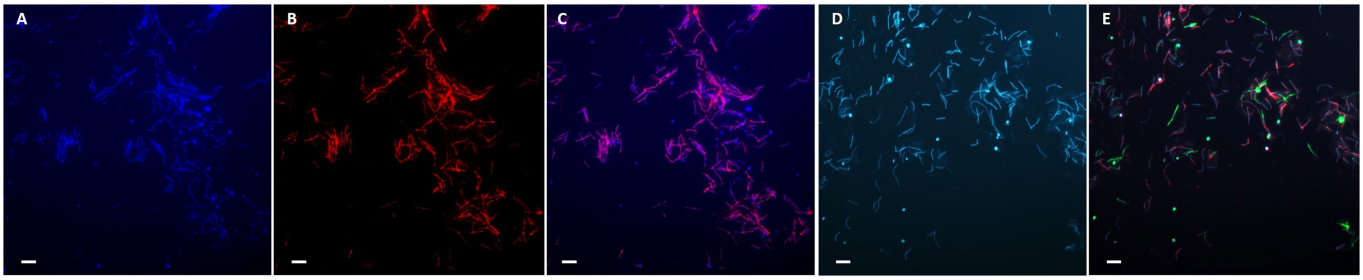

Extended Data Fig. 4 | Representative fluorescence micrographs of culture LCB3. A. Cells visualized with DAPI (blue). **B**. Cells visualized by DOPE-FISH using a '*Ca*. M. washburnensis' specific 16S rRNA-targeted oligonucleotide probe (KRmw515, red). **C**. Overlay of A and B. **D**. Cells visualized with DAPI (blue). **E**. Cells visualized with DAPI (blue, same field of view as in D) combined with dual CARD-FISH using the '*Ca*. M. washburnensis' specific 16S rRNA-targeted oligonucleotide probe (KRmw515, red) and a general archaea probe (Arch915, green). Note that because of two mismatches of the Arch915 probe to the 16S rRNA of '*Ca*. M. washburnensis' there is no overlap of signal from probes KRmw515 and Arch915. Representative micrographs from n = 3 independent samples from culture LCB3. Scale bars 5 µm.

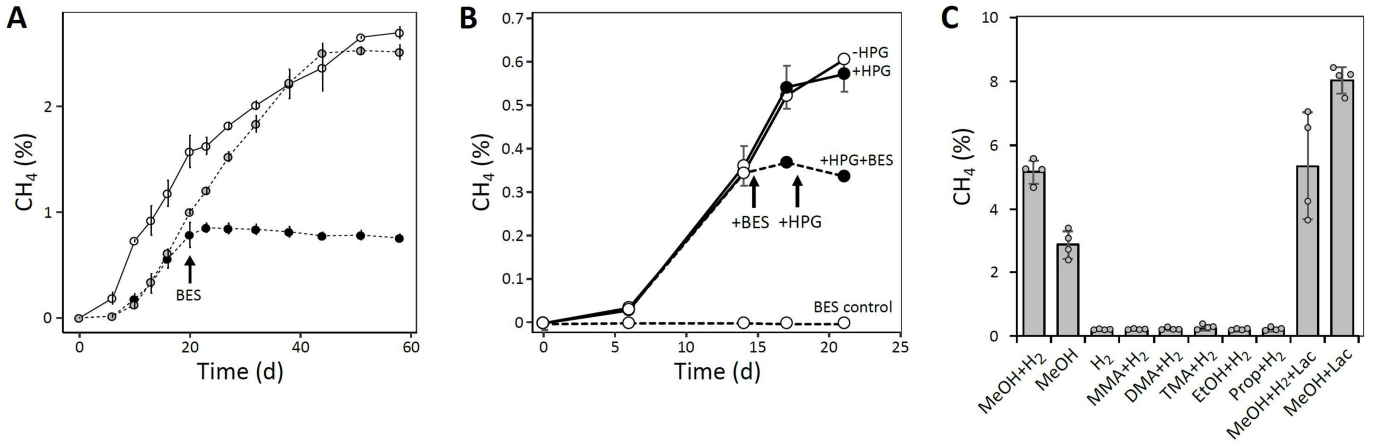

Extended Data Fig. 5 | Methane production in culture LCB3 under different experimental conditions. A. Methane production curves for SIP incubations (shown in Fig. 1b) amended with ^{12}C-methanol (open white circles), ^{13}C-methanol (gray filled circles), or ^{13}C-methanol with BES (black filled circles). Data are presented as mean values +/− standard deviation (n = 3 biological replicates). **B**. Methane production curves for BONCAT-FISH incubations (shown in Fig. 3c) amended with methanol and hydrogen, spiked with BES at day 15 (filled symbols, dashed line) and spiked with HPG at day 18 (filled symbols). Controls were not spiked (open symbols), representing growth under standard cultivation conditions, or were spiked with BES at day 0 (open symbols, dashed line), inhibiting methane production. Incubations were sampled for cell visualization via BONCAT-FISH after 24 h of incubation with HPG (day 19). Data are presented as mean values +/− standard deviation (n = 3 biological replicates). **C**. Methane produced with different substrates after 85 days of incubation. Concentrations were 10 mM for methanol (MeOH), monomethylamine (MMA), dimethylamine (DMA), trimethylamine (TMA), ethanol (EtOH), and isopropanol (Prop); 2mM for lactate (Lac); and 50% for hydrogen (H_2).

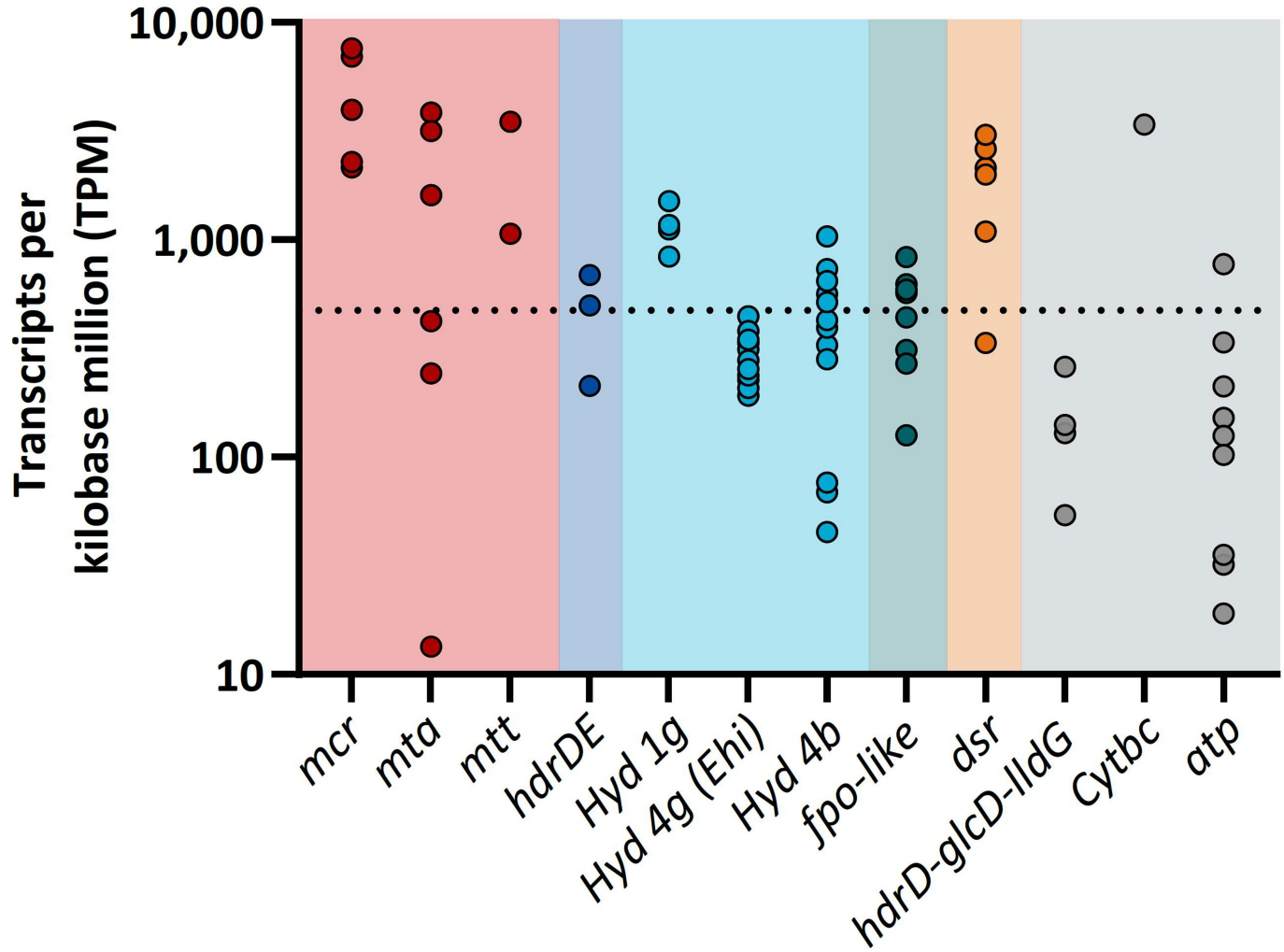

Extended Data Fig. 6 | Gene expression of '*Ca*. M. washburnensis' strain LCB3 during methanogenic growth on hydrogen and methanol. Dashed line represents the average transcripts per kilobase million (TPM) of all genes (n = 1 experiment). Each dot represents the expression of a subunit in a multi-subunit enzyme complex. For abbreviations see Fig. 4. See SI Tables 10, 11 for details on gene annotation and gene expression.

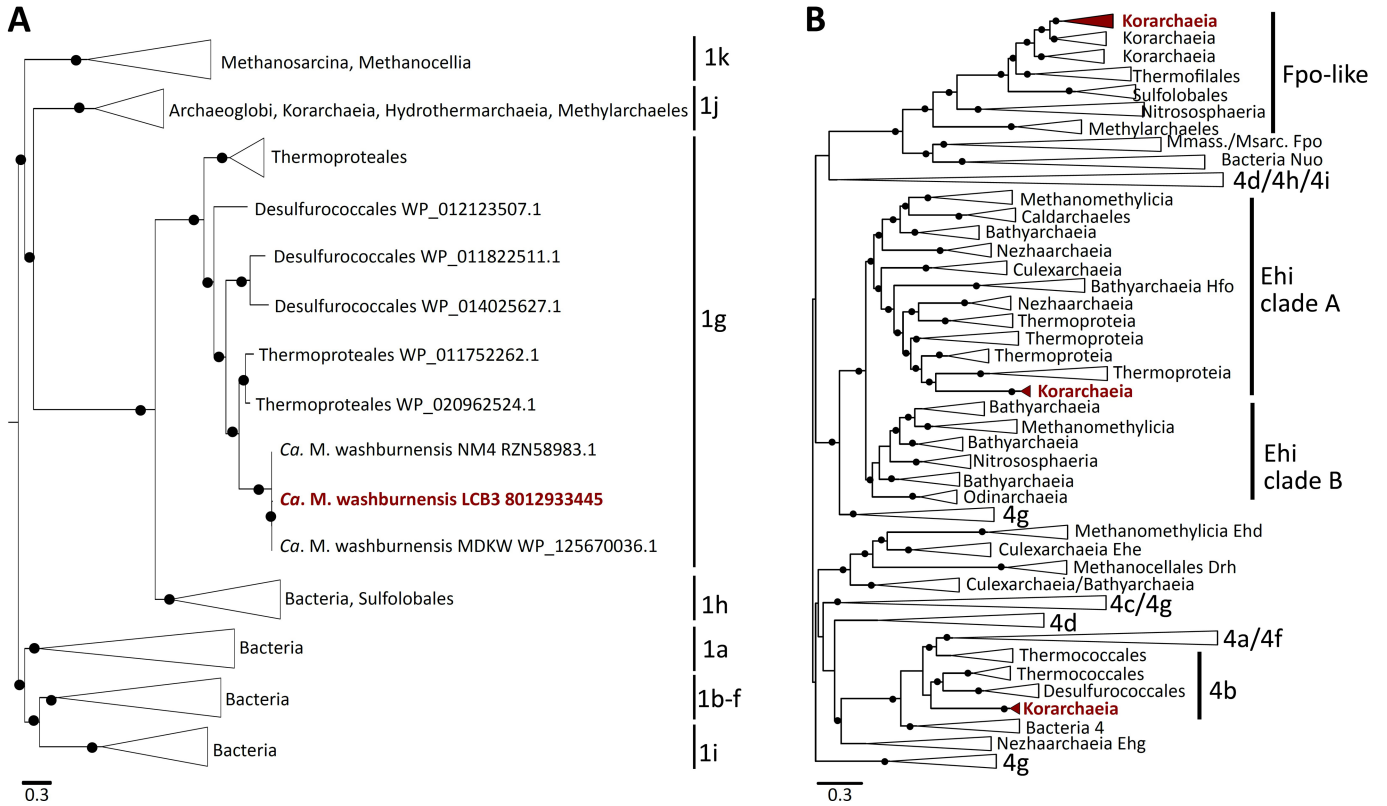

Extended Data Fig. 7 | Phylogenetic classification of [NiFe]-hydrogenases in '*Ca*. M. washburnensis' strain LCB3. A. Maximum likelihood phylogenetic tree of group 1 [NiFe]-hydrogenases. The tree was constructed using IQtree2 with the best fit model LG+R10 and 1000 ultrafast bootstraps. Hydrogenase classes were assigned according to the HydDB. The sequence from the LCB3 genome is highlighted in red. Black circles indicate ultrafast bootstrap values >95. **B**. Maximum likelihood phylogenetic tree of group 4 [NiFe]-hydrogenases. The tree was constructed using IQtree2 with the best fit model LG+R10 and 1000 ultrafast bootstraps. Clades containing sequences from the LCB3 genome are highlighted in red. Black circles indicate ultrafast bootstrap values >95.

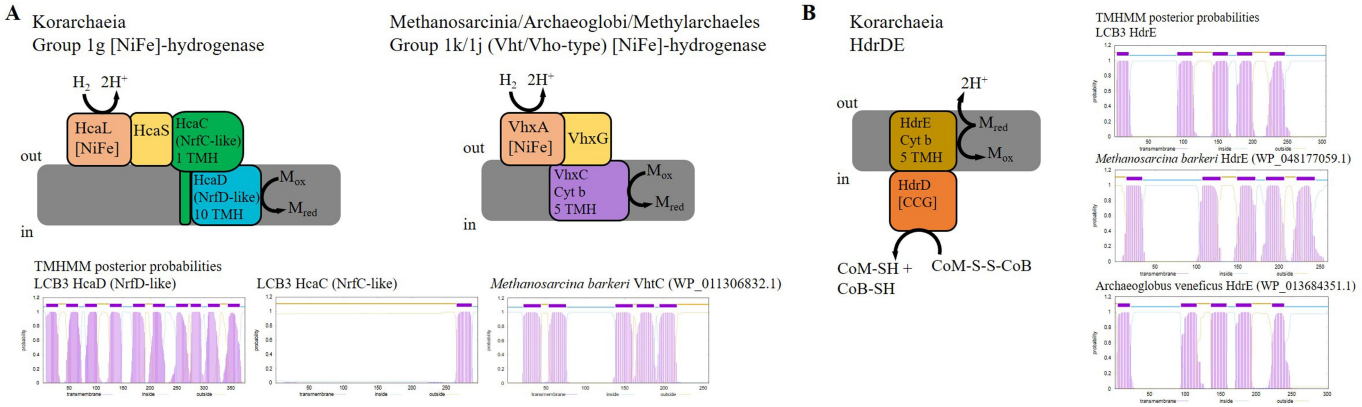

Extended Data Fig. 8 | Annotation of enzyme complexes in '*Ca*. M. washburnensis' strain LCB3. A. Comparison of group 1 [NiFe]-hydrogenase organization and structure between '*Ca*. M. washburnensis' strain LCB3 and other MCR-encoding archaeal lineages. Models of the enzyme arrangement in the membrane with matching colors between the models indicating conserved function. Transmembrane helix (TMH) probabilities for intermembrane subunits. Groups 1j/1k have b-type cytochrome containing subunits with five helices, while the Korarchaeia group 1g [NiFe]-hydrogenase has an NrfD-like subunit (HcaC) with ten helices and lacks b-type cytochromes. **B**. Annotation of the '*Ca*. M. washburnensis' strain LCB3 HdrDE complex. Model representing the arrangement of genes in the membrane. All HdrE subunits analyzed have 5 TMHs. The HdrD subunit in the LCB3 genome has cysteine residues that are conserved in HdrD subunits from other lineages. Transmembrane helices were predicted using the TMHMM 2.0 server.

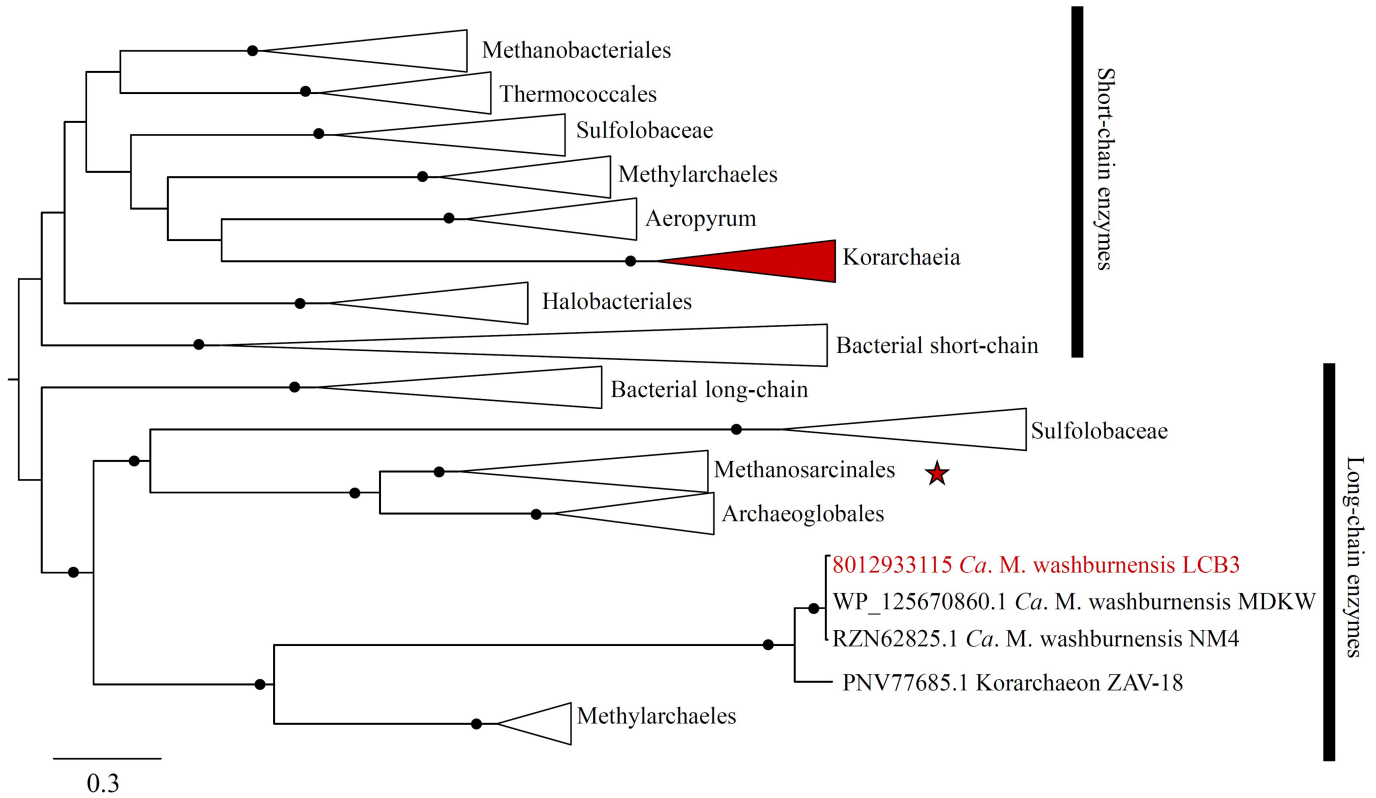

Extended Data Fig. 9 | Phylogenetic tree of geranylfarnesyl diphosphate synthase homologs in archaea and bacteria. Red clades and text correspond to homologs encoded in '*Ca*. M. washburnensis' strain LCB3. Red star indicates the clade containing the *Methanosarcina mazei* homolog involved in methanophenazine biosynthesis. Circles represent ultrafast bootstrap values >95. Short-chain and long-chain designations according to Ou et al.[73].